



**Fermi National Accelerator Laboratory**

**FERMILAB-Pub-99/093-E**

**KTeV**

**Light Gluino Search for Decays Containing  $\pi^+\pi^-$  or  $\pi^0$  from a  
Neutral Hadron Beam at Fermilab**

A. Alavi-Harati et al.  
The KTeV Collaboration

*Fermi National Accelerator Laboratory  
P.O. Box 500, Batavia, Illinois 60510*

April 1999

Submitted to *Physical Review Letters*

## **Disclaimer**

*This report was prepared as an account of work sponsored by an agency of the United States Government. Neither the United States Government nor any agency thereof, nor any of their employees, makes any warranty, expressed or implied, or assumes any legal liability or responsibility for the accuracy, completeness, or usefulness of any information, apparatus, product, or process disclosed, or represents that its use would not infringe privately owned rights. Reference herein to any specific commercial product, process, or service by trade name, trademark, manufacturer, or otherwise, does not necessarily constitute or imply its endorsement, recommendation, or favoring by the United States Government or any agency thereof. The views and opinions of authors expressed herein do not necessarily state or reflect those of the United States Government or any agency thereof.*

## **Distribution**

*Approved for public release; further dissemination unlimited.*

## **Copyright Notification**

*This manuscript has been authored by Universities Research Association, Inc. under contract No. DE-AC02-76CHO3000 with the U.S. Department of Energy. The United States Government and the publisher, by accepting the article for publication, acknowledges that the United States Government retains a nonexclusive, paid-up, irrevocable, worldwide license to publish or reproduce the published form of this manuscript, or allow others to do so, for United States Government Purposes.*

# Light Gluino Search for Decays Containing $\pi^+\pi^-$ or $\pi^0$ from a Neutral Hadron Beam at Fermilab.

A. Alavi-Harati<sup>12</sup>, I.F. Albuquerque<sup>10</sup>, T. Alexopoulos<sup>12</sup>, M. Arenton<sup>11</sup>, K. Arisaka<sup>2</sup>,  
S. Averitte<sup>10</sup>, A.R. Barker<sup>5</sup>, L. Bellantoni<sup>7</sup>, A. Bellavance<sup>9</sup>, J. Belz<sup>10</sup>, R. Ben-David<sup>7</sup>,  
D.R. Bergman<sup>10</sup>, E. Blucher<sup>4</sup>, G.J. Bock<sup>7</sup>, C. Bown<sup>4</sup>, S. Bright<sup>4</sup>, E. Cheu<sup>1</sup>, S. Childress<sup>7</sup>,  
R. Coleman<sup>7</sup>, M.D. Corcoran<sup>9</sup>, G. Corti<sup>11</sup>, B. Cox<sup>11</sup>, M.B. Crisler<sup>7</sup>, A.R. Erwin<sup>12</sup>,  
R. Ford<sup>7</sup>, A. Golossanov<sup>11</sup>, G. Graham<sup>4</sup>, J. Graham<sup>4</sup>, K. Hagan<sup>11</sup>, E. Halkiadakis<sup>10</sup>,  
K. Hanagaki<sup>8</sup>, S. Hidaka<sup>8</sup>, Y.B. Hsiung<sup>7</sup>, V. Jejer<sup>11</sup>, J. Jennings<sup>2</sup>, D.A. Jensen<sup>7</sup>,  
R. Kessler<sup>4</sup>, H.G.E. Kobrak<sup>3</sup>, J. LaDue<sup>5</sup>, A. Lath<sup>10,†</sup>, A. Ledovskoy<sup>11</sup>, P.L. McBride<sup>7</sup>,  
A.P. McManus<sup>11</sup>, P. Mikelsons<sup>5</sup>, E. Monnier<sup>4,\*</sup>, T. Nakaya<sup>7</sup>, U. Nauenberg<sup>5</sup>, K.S. Nelson<sup>11</sup>,  
H. Nguyen<sup>7</sup>, V. O'Dell<sup>7</sup>, M. Pang<sup>7</sup>, R. Pordes<sup>7</sup>, V. Prasad<sup>4</sup>, C. Qiao<sup>4</sup>, B. Quinn<sup>4</sup>,  
E.J. Ramberg<sup>7</sup>, R.E. Ray<sup>7</sup>, A. Roodman<sup>4</sup>, M. Sadamoto<sup>8</sup>, S. Schnetzer<sup>10</sup>, K. Senyo<sup>8</sup>,  
P. Shanahan<sup>7</sup>, P.S. Shawhan<sup>4</sup>, W. Slater<sup>2</sup>, N. Solomey<sup>4</sup>, S.V. Somalwar<sup>10</sup>, R.L. Stone<sup>10</sup>,  
I. Suzuki<sup>8</sup>, E.C. Swallow<sup>4,6</sup>, R.A. Swanson<sup>3</sup>, S.A. Taegar<sup>1</sup>, R.J. Tesarek<sup>10</sup>, G.B. Thomson<sup>10</sup>,  
P.A. Toale<sup>5</sup>, A.K. Tripathi<sup>2</sup>, R. Tschirhart<sup>7</sup>, Y.W. Wah<sup>4</sup>, J. Wang<sup>1</sup>, H.B. White<sup>7</sup>,  
J. Whitmore<sup>7</sup>, B. Winstein<sup>4</sup>, R. Winston<sup>4</sup>, J.-Y. Wu<sup>5</sup>, T. Yamanaka<sup>8</sup>, E.D. Zimmerman<sup>4</sup>

(KTeV Collaboration)

<sup>1</sup> *University of Arizona, Tucson, Arizona 85721*

<sup>2</sup> *University of California at Los Angeles, Los Angeles, California 90095*

<sup>3</sup> *University of California at San Diego, La Jolla, California 92093*

<sup>4</sup> *The Enrico Fermi Institute, The University of Chicago, Chicago, Illinois 60637*

<sup>5</sup> *University of Colorado, Boulder, Colorado 80309*

<sup>6</sup> *Elmhurst College, Elmhurst, Illinois 60126*

<sup>7</sup> *Fermi National Accelerator Laboratory, Batavia, Illinois 60510*

<sup>8</sup> *Osaka University, Toyonaka, Osaka 560 Japan*

<sup>9</sup> *Rice University, Houston, Texas 77005*

<sup>10</sup> *Rutgers University, Piscataway, New Jersey 08855*

<sup>11</sup> *University of Virginia, Charlottesville, Virginia 22901*

<sup>12</sup> *University of Wisconsin, Madison, Wisconsin 53706*

## Abstract

We report on two null searches, one for the spontaneous appearance of  $\pi^+\pi^-$  pairs, another for a single  $\pi^0$ , consistent with the decay of a long-lived neutral particle into hadrons and an unseen neutral particle. For the lowest level gluon-gluino bound state, known as the  $R^0$ , we exclude the decays  $R^0 \rightarrow \pi^+\pi^-\tilde{\gamma}$  and  $R^0 \rightarrow \pi^0\tilde{\gamma}$  for the masses of  $R^0$  and  $\tilde{\gamma}$  in the theoretically allowed range. In the most interesting  $R^0$  mass range,  $\leq 3 \text{ GeV}/c^2$ , we exclude  $R^0$  lifetimes from  $3 \times 10^{-10}$  seconds to as high as  $10^{-3}$  seconds, assuming perturbative QCD production for the  $R^0$ .

PACS numbers: 13.85.Rm, 13.25.Es, 14.40.Aq, 14.80.Ly

Light masses for gluinos ( $\tilde{g}$ ) and photinos ( $\tilde{\gamma}$ ) arise naturally in many supersymmetry (SUSY) models, including those that solve the SUSY-CP problem by eliminating dimension-3 operators [1]. They predict light gauginos and heavy squarks, and have not been ruled out conclusively. In such models the gluino and photino masses are expected to be  $\leq 1.0 \text{ GeV}/c^2$ . The gluino should form bound states with normal quarks and gluons ( $g$ ), the lightest of which is called the  $R^0$ , a spin  $1/2$   $g\tilde{g}$  bound state.

Estimates of the mass and lifetime of the  $R^0$  vary from 1 to 3  $\text{GeV}/c^2$  and  $10^{-10}$  to  $10^{-5}$  s respectively [2]. Chung, Farrar, and Kolb [3] show that a stable  $\tilde{\gamma}$  as a relic dark matter candidate requires the ratio of masses  $M_{R^0}/M_{\tilde{\gamma}} \equiv r$  to be  $1.3 \leq r \leq 1.8$ . The range  $1.3 \leq r \leq 1.55$  is favored. Values of  $r$  below 1.3 yield an insufficient abundance of dark matter, while too large a value of  $r$  overcloses the universe. A previous direct search for the  $R^0$  by the KTeV collaboration is described in [4]. That result, based on 5% of the data collected by the KTeV experiment in 1996, excluded the  $R^0$  with the constraint  $M_{R^0} - M_{\tilde{\gamma}} \geq 0.648 \text{ GeV}/c^2$ . Thus for  $r \leq 1.4$ , our previous result was insensitive to  $M_{R^0} \leq 2.3 \text{ GeV}/c^2$ , which represents a large portion of the region of primary interest [5]. A search for the C-suppressed decay  $R^0 \rightarrow \eta\tilde{\gamma}$  is discussed in [6]. References to other searches can be found in [4].

We assume exactly the same production mechanism and rates as described in [4]. The  $R^0$  is expected to decay mainly into  $\rho\tilde{\gamma}$ . The decay into  $\pi^0\tilde{\gamma}$  or  $\eta\tilde{\gamma}$  is suppressed due to conservation of  $C$ -parity. Figure 1 illustrates the lower limit of sensitivity in  $M_{R^0} - M_{\tilde{\gamma}}$  of the three decay modes mentioned above, along with the cosmological constraints. We report on null searches for two decay modes. The first is the dominant decay,  $R^0 \rightarrow \rho\tilde{\gamma}$ ,  $\rho \rightarrow \pi^+\pi^-$ . The second is the  $C$ -violating decay  $R^0 \rightarrow \pi^0\tilde{\gamma}$ . In both decays, the  $\tilde{\gamma}$  escapes undetected.

The KTeV experiment as used in the  $R^0$  search is described in [4]. The data used in the  $R^0 \rightarrow \rho\tilde{\gamma}$ ,  $\rho \rightarrow \pi^+\pi^-$  analysis were collected during the 1996 run of KTeV (FNAL E832). The trigger and analysis cuts used are similar to those described in [4]. To detect a possible  $R^0$  signal we examined decays with two charged particles; specifically the shape of the invariant mass distribution, with the assumption that the particles were pions ( $M_{\pi^+\pi^-}$ ).

An online filter was used during data collection to classify the events according to  $\pi^+\pi^-$  invariant mass. The data with  $M_{\pi^+\pi^-} < 0.45 \text{ GeV}/c^2$  were prescaled. Backgrounds consisted of  $K_L \rightarrow \pi^\pm l^\mp \nu$  ( $l = e, \mu$ ) decays with leptons mis-identified as pions (semi-leptonic decays);  $K_L \rightarrow \pi^+\pi^-$  and  $K_L \rightarrow \pi^+\pi^-\gamma$  decays; as well as  $K_L \rightarrow \pi^+\pi^-\pi^0$  decays with undetected  $\pi^0$ 's.

The offline analysis, including cuts using photon veto energies, semileptonic decay rejection, and track, vertex quality requirements, was similar to that described in [4]. Additional cuts reduced the probability of track reconstruction errors that paired the wrong combination of horizontal and vertical track components. The  $K_L \rightarrow \pi^+\pi^-$  decays were rejected by requiring the square of the transverse momentum of the  $\pi^+\pi^-$  with respect to the beam direction ( $P_T^2$ ) to be greater than  $0.001 \text{ (GeV}/c)^2$ , and the  $K_L \rightarrow \pi^+\pi^-\gamma$  and  $K_L \rightarrow \pi^+\pi^-\pi^0$  decays were rejected by using the calorimeter to identify the photons from respective decays. In the region  $M_{\pi^+\pi^-} \leq 0.36 \text{ GeV}/c^2$  additional cuts ( $K_L \rightarrow \pi^+\pi^-\pi^0$  specific cuts), including restricting the total energy deposited in the calorimeter to  $\leq 5 \text{ GeV}/c^2$ , further reduced the  $K_L \rightarrow \pi^+\pi^-\pi^0$  decays.

We performed a maximum-likelihood fit to the  $M_{\pi^+\pi^-}$  distribution, using Monte Carlo distributions for  $K_L \rightarrow \pi e \nu$ ,  $K_L \rightarrow \pi \mu \nu$ ,  $K_L \rightarrow \pi^+\pi^-$ ,  $K_L \rightarrow \pi^+\pi^-\pi^0$ , and  $R^0 \rightarrow \pi^+\pi^-\tilde{\gamma}$ . The Monte Carlo events were subjected to all the same cuts as the data, however the  $e^\pm$  identification cuts was not applied to the  $K_L \rightarrow \pi e \nu$ , and a muon veto requirement was not required for the  $K_L \rightarrow \pi \mu \nu$  events. These lepton identification cuts have no effect on the  $M_{\pi^+\pi^-}$  distribution. The amplitudes for all the simulated  $M_{\pi^+\pi^-}$  shapes were allowed to vary independently.

Figure 2(a) shows the  $M_{\pi^+\pi^-}$  distribution for all data, before applying the  $K_L \rightarrow \pi^+\pi^-\pi^0$  specific and  $P_T^2$  cuts. There are  $\sim 2.1 \times 10^6$  CP-violating  $K_L \rightarrow \pi^+\pi^-$  decays in the peak at  $M_K$ . The sharp edge at  $M_{\pi^+\pi^-} = 0.45 \text{ GeV}/c^2$  is due to the online filter prescale. The  $K_L \rightarrow \pi^+\pi^-\pi^0$  decays are evident at  $M_{\pi^+\pi^-} \leq 0.36 \text{ GeV}/c^2$ , and the kinematic limit is evident at  $2M_\pi = 0.28 \text{ GeV}/c^2$ . Also shown in Figure 2(a) is the sum of the various kaon decay distributions from Monte Carlo. The data and kaon decay simulation are in agreement

for six orders of magnitude. In addition, the  $P_T^2$  distributions for data and sum of decay simulations (not shown) are in good agreement, using the amplitudes for the various kaon decays found in  $M_{\pi^+\pi^-}$  fit.

Figure 2(b) shows the  $M_{\pi^+\pi^-}$  distribution for the data with all the cuts, as well as the sum of the  $K_L$  decay simulations, and distributions for two sample  $R^0, \tilde{\gamma}$  combinations. The  $K_L \rightarrow \pi^+\pi^-$  peak in data is significantly reduced due to the  $P_T^2$  cut. The agreement between data and the sum of  $K_L$  decay simulations has an overall  $\chi^2/\text{degree of freedom}$  of  $\sim 194/148$  for the region  $0.28 \text{ GeV}/c^2 \leq M_{\pi^+\pi^-} \leq 0.58 \text{ GeV}/c^2$ .

The two sample  $R^0$  distributions shown in figure 2(b), are scaled to the expected rate [7] [8] for  $R^0$ 's with a lifetime equal to the lifetime of the  $K_L$ . Since the shape due to  $R^0$  decay is significantly different from those due to kaon decay, we searched for the  $R^0$  by examining the difference between the  $M_{\pi^+\pi^-}$  shape and the shape expected from kaon decays. The data show no deviation in the  $M_{\pi^+\pi^-}$  shape that could indicate a contribution from an  $R^0$  decay. Limits on  $R^0$  were obtained using the maximum likelihood fit explained above. There are 10 events with  $M_{\pi^+\pi^-} \geq 0.6 \text{ GeV}/c^2$  that are not simulated by  $K_L$  decays. These events, which are consistent with residual gas interactions in the vacuum, are treated as signal in the fit.

Various  $R^0, \tilde{\gamma}$  combinations, with  $1.3 \leq r \leq 2.2$  were used in the fit. All fits yielded  $R^0$  components consistent with zero. An upper limit for a given  $R^0$  was determined by evaluating the maximum-likelihood curve at the 90% confidence level (C.L.) interval, which limited the  $R^0$  decays to less than a few tens to hundreds range. The detector acceptance and the  $R^0$  flux at production were then determined as a function of the  $R^0$  lifetime. The normalization was performed using  $2.1 \times 10^6$   $K_L \rightarrow \pi^+\pi^-$  events observed, from which we determined that  $37.7 \times 10^{10}$   $K^0$  exited the absorbers [4]. Figure 3 shows the 90% C.L. upper limit on the ratio  $R^0/K^0$ , as well as the expectation for the  $R^0/K^0$  ratio for  $r = 1.4$ .

Figure 4 shows the variation of the 90% C.L. upper limit on the  $R^0/K^0$  flux ratio with the  $R^0$  lifetime for two sample  $R^0, \tilde{\gamma}$  combinations. Particles with lifetimes much shorter than the  $K_L$  decay too close to the target to be visible in the detector, while those with much longer

lifetimes exit the detector without decaying. We use the  $R^0/K^0$  flux expectation to exclude a range of lifetimes for a given  $R^0$ ,  $\tilde{\gamma}$  combination. Figure 5 shows  $R^0$  lifetimes excluded at 90% C.L. for a given mass, assuming a 100% branching fraction for the  $R^0 \rightarrow \pi^+\pi^-\tilde{\gamma}$  decay. Contours are shown for  $r = 1.3, 1.4, 1.55, 1.73$ .

In this analysis, we are able to exclude  $R^0$ 's with masses well below the lower limits of previous searches ( $\sim 2.2 \text{ GeV}/c^2$ ). The lower limit of the exclusion contour (at  $1.3 \text{ GeV}/c^2$  for  $r = 1.3$ ) is due to the kinematic limit of  $M_{R^0} - M_{\tilde{\gamma}} = 2M_\pi$ . We note that in the theoretically interesting regions of  $M_{R^0}$  and  $r$ , our exclusion covers lifetimes as low as  $3 \times 10^{-10}$  seconds, and as high as  $10^{-3}$  seconds, effectively spanning the theoretically interesting range of lifetimes.

If the mass difference  $M_{R^0} - M_{\tilde{\gamma}}$  is less than  $2M_\pi$  then the  $R^0$  can only decay via  $R^0 \rightarrow \pi^0\tilde{\gamma}$ . We searched for the decay  $R^0 \rightarrow \pi^0\tilde{\gamma}$ ,  $\pi^0 \rightarrow \gamma\gamma$  in data taken during a special run whose primary purpose was to search for the decay  $K_L \rightarrow \pi^0\nu\bar{\nu}$  [9]. Since the signatures for the  $K_L$  and  $R^0$  decays, two photons with missing transverse momentum ( $P_T$ ), are similar, these data are sensitive to  $R^0 \rightarrow \pi^0\tilde{\gamma}$  decays.

Only one narrow beam of neutral kaons was used in this run, with the transverse beam size of  $4 \text{ cm} \times 4 \text{ cm}$  at the calorimeter. The trigger was designed to select events with two energy clusters in the calorimeter, together with four cluster events ( $K_L \rightarrow \pi^0\pi^0$ ) for normalization. The longitudinal distance of the decay vertex from the target ( $Z$ ) and the transverse momentum of the two photons were determined by constraining the invariant mass of the two photons to that of  $\pi^0$ . The average  $P_T$  resolution was  $\sim 8 \text{ MeV}/c$ . The selection criteria used in this data sample are similar to the one used in the  $\pi^0\nu\bar{\nu}$  analysis [9], with the exception of the  $P_T$  cut at  $260 \text{ MeV}/c$ . Photon veto detectors and drift chambers were used to suppress backgrounds from other kaon decays and hadronic interactions in the detector. The events were required to have the decay vertex in vacuum, with the vertex  $Z$  position in the range  $125 \leq Z \leq 157 \text{ m}$ .

We examined the shape of the  $P_T$  distribution to isolate  $R^0$  candidates. The  $P_T$  distribution of the final data sample is shown in Figure 6, along with the background expected

from  $K_L \rightarrow \gamma\gamma$  and  $\Lambda \rightarrow n\pi^0$  decays. The peak near  $P_T = 0$  is from the decay  $K_L \rightarrow \gamma\gamma$ , and the remaining events below  $P_T = 160$  MeV/ $c$  are from  $\Lambda$  decays. The signal search region at  $P_T > 160$  MeV/ $c$ , chosen to minimize background from hyperon and  $K_L$  decays, is indicated by the arrow. Clearly, we are sensitive to  $R^0$  masses for which the  $\pi^+\pi^-$  decay cannot proceed.

After all cuts, two events remain in the signal region. From studies of  $\Lambda \rightarrow n\pi^0$  decays [9], we expect the number of events from hadronic interactions to be  $4.7 \pm 1$ , consistent with the number of events remaining in our sample. Treating these two events as signal, the corresponding 90% C.L. upper limit on the number of observed  $R^0$  signal events is 5.32.

The  $K_L$  flux in this data sample was measured from 3466 observed  $K_L \rightarrow \pi^0\pi^0$  decays. The pQCD prediction for the  $R^0/K_L$  flux ratio were used as before to obtain upper and lower lifetime limits at the 90% C.L., assuming the  $R^0$  decays 100% of the time to  $\pi^0\tilde{\gamma}$ . Figure 7 shows the exclusion contours for  $r = 1.3$ , and  $r = 1.4$  using the  $\pi^0$  analysis, and the  $\pi^+\pi^-$  analysis. Note that using the  $\pi^0$  analysis, we extend the range of excluded  $M_{R^0}$  down to 0.8 GeV/ $c^2$ , for lifetimes between  $2.5 \times 10^{-10}$  and  $5.6 \times 10^{-6}$  seconds.

The analyses presented in this paper exclude most  $R^0$  masses, over six decades in lifetime. A significant portion of the region allowed by the cosmological constraint  $r \leq 1.4$  and  $M_{R^0} \leq 2.2$  GeV/ $c^2$  which was not addressed by previous searches is now excluded. We thus definitively close the light gaugino window. Our null results eliminate most SUSY models in which gauginos remain massless at tree-level. More generally, our understanding of the  $M_{\pi^+\pi^-}$  shape will constrain future models that predict long-lived particles with a  $\pi^+\pi^-$  component in their decays.

We thank Glennys Farrar for suggesting this search and for discussions concerning this work and, along with Rocky Kolb, for pointing out the cosmological significance of this search. We gratefully acknowledge the support and effort of the Fermilab staff and the technical staffs of the participating institutions for their vital contributions. This work was supported in part by the U.S. DOE, The National Science Foundation and The Ministry of Education and Science of Japan. In addition, A.R.B., E.B. and S.V.S. acknowledge support

from the NYI program of the NSF; A.R.B. and E.B. from the Alfred P. Sloan Foundation; E.B. from the OJI program of the DOE; K.H., T.N. and M.S. from the Japan Society for the Promotion of Science. P.S.S. acknowledges receipt of a Grainger Fellowship.

## REFERENCES

<sup>†</sup> To whom correspondence should be addressed.

Electronic address: lath@physics.rutgers.edu

\* On leave from C.P.P. Marseille/C.N.R.S., France.

- [1] R. Mohapatra and S. Nandi, Phys. Rev. Lett. **79**, 181 (1997); Z. Chacko et al., Phys. Rev. D**56**, 5466 (1997); S. Raby, Phys. Rev. D**56**, 2852 (1997).
- [2] G.R. Farrar, Phys. Rev. Lett. **76**, 4111 (1996); G.R. Farrar, Phys. Rev. D **51**, 3904 (1995);
- [3] D.J.H. Chung, G.R. Farrar, and E.W. Kolb, Phys Rev. D **56**, 6096 (1997); G.R. Farrar and E.W. Kolb, Phys. Rev. D **53**, 2990 (1996).
- [4] J. Adams *et al.*, Phys Rev. Lett **79**, 4083 (1997).
- [5] G. R. Farrar, Nucl. Phys. Proc. Suppl. **62**, 485 (1998) (available as eprint hep-ph/9710277).
- [6] V. Fanti *et al.* Phys. Lett. B **446**, 117 (1999).
- [7] S. Dawson, E. Eichten, and C. Quigg, Phys. Rev. D **31**, 1581 (1985).
- [8] C. Quigg (private communication).
- [9] J. Adams *et al.*, Phys. Lett. B **447**, 240 (1999).

FIGURES

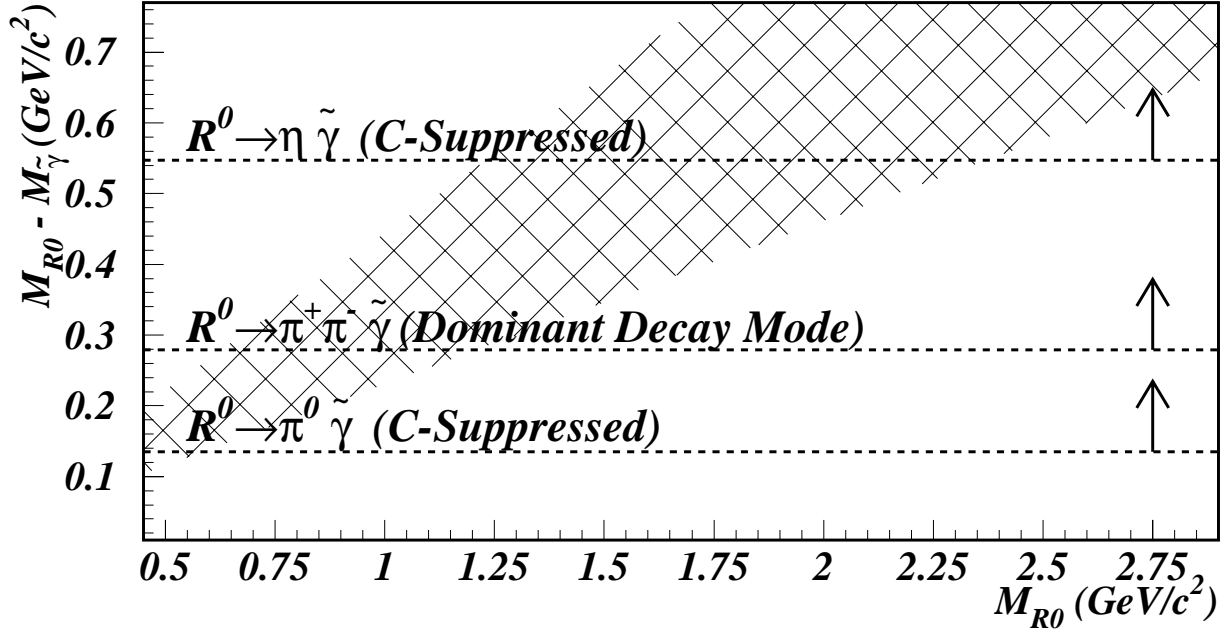


FIG. 1.  $M_{R^0} - M_{\tilde{\gamma}}$  vs.  $M_{R^0}$ , showing the region allowed by cosmological arguments,  $1.3 \leq r \leq 1.8$  (hatched). The dashed lines represent the lowest level of sensitivity for the various decay modes.

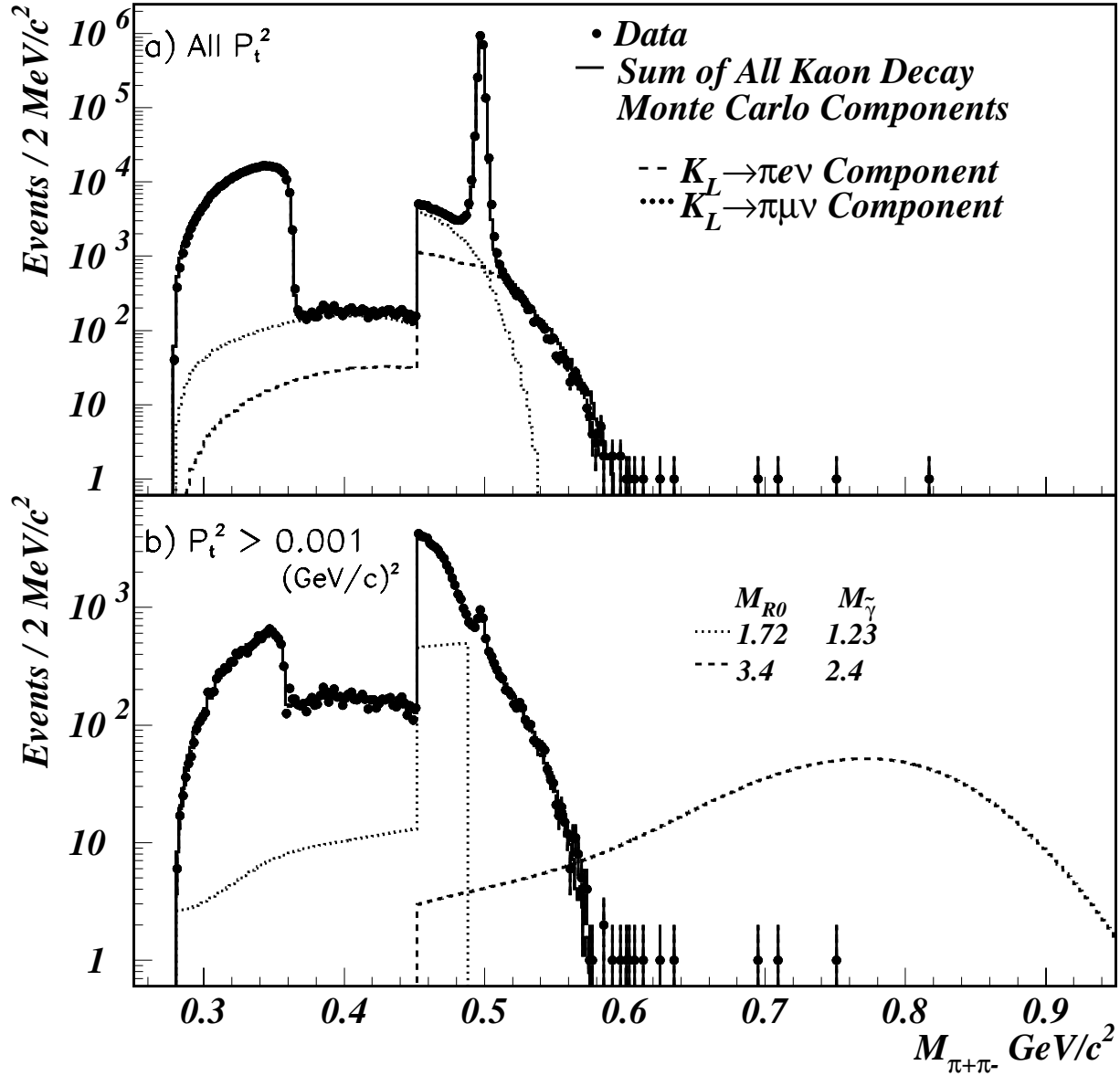


FIG. 2.  $M_{\pi^+\pi^-}$  distribution with all but  $P_t^2$  and  $K_L \rightarrow \pi^+\pi^-\pi^0$  specific cuts (a), and all cuts (b). The data (dots), sum of all MC (solid line) are shown. Suppression below  $0.45 \text{ GeV}/c^2$  is due to the online filter prescale. The separate contributions from semileptonic decays (dashed and dotted lines) are also shown in (a). Distributions due to two sample  $R^0$ 's of lifetime  $5 \times 10^{-8}$  sec using the predicted flux (dashed and dotted lines) are also shown in (b).

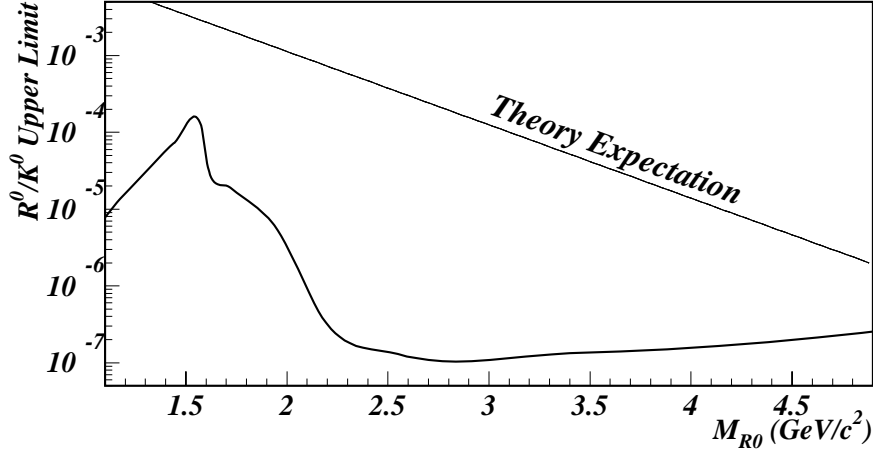


FIG. 3. The 90% C.L. upper limit on the  $R^0/K^0$  ratio, and the expectation, for  $r = 1.4$ ,  $\tau(R^0) = 5 \times 10^{-8}$  sec.

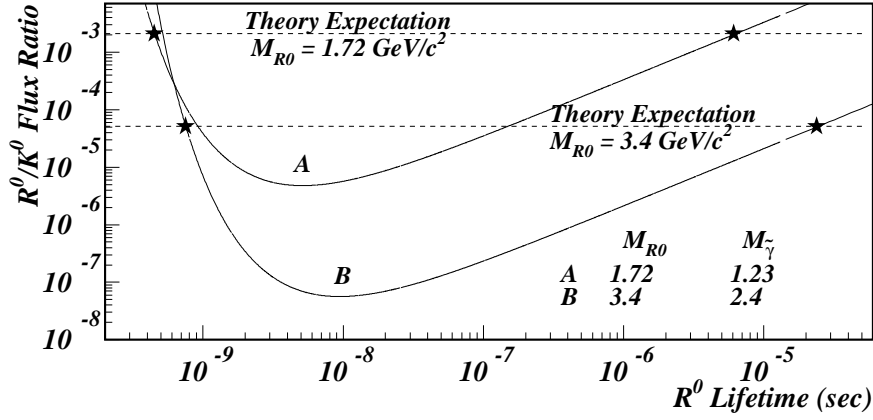


FIG. 4. Upper limits with 90% C.L. on the  $R^0/K^0$  flux ratio as a function of  $R^0$  lifetime, for two  $M_{R^0}$ ,  $M_{\tilde{\gamma}}$  combinations, with masses listed in  $\text{GeV}/c^2$ . The dotted lines show the expectation for the flux ratio, and the stars mark the corresponding lifetime limits.

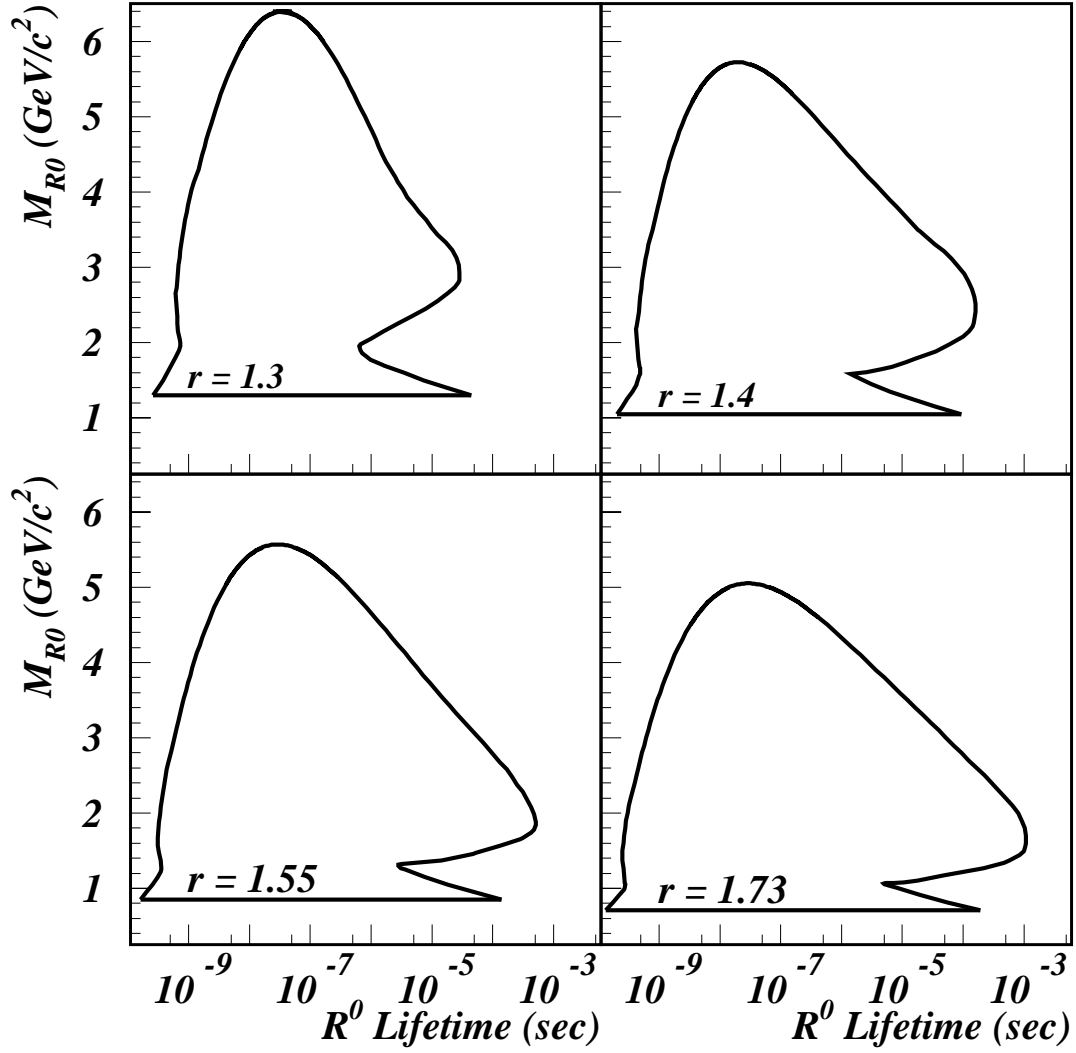


FIG. 5.  $R^0$  mass-lifetime regions excluded at 90% C.L., for the decay  $R^0 \rightarrow \pi^+ \pi^- \tilde{\gamma}$ , for values of  $r = 1.3, 1.4, 1.55,$  and  $1.73$ . The lower edges are due to the kinematic limit of  $M_{R^0} - M_{\tilde{\gamma}} = 2M_\pi$ .

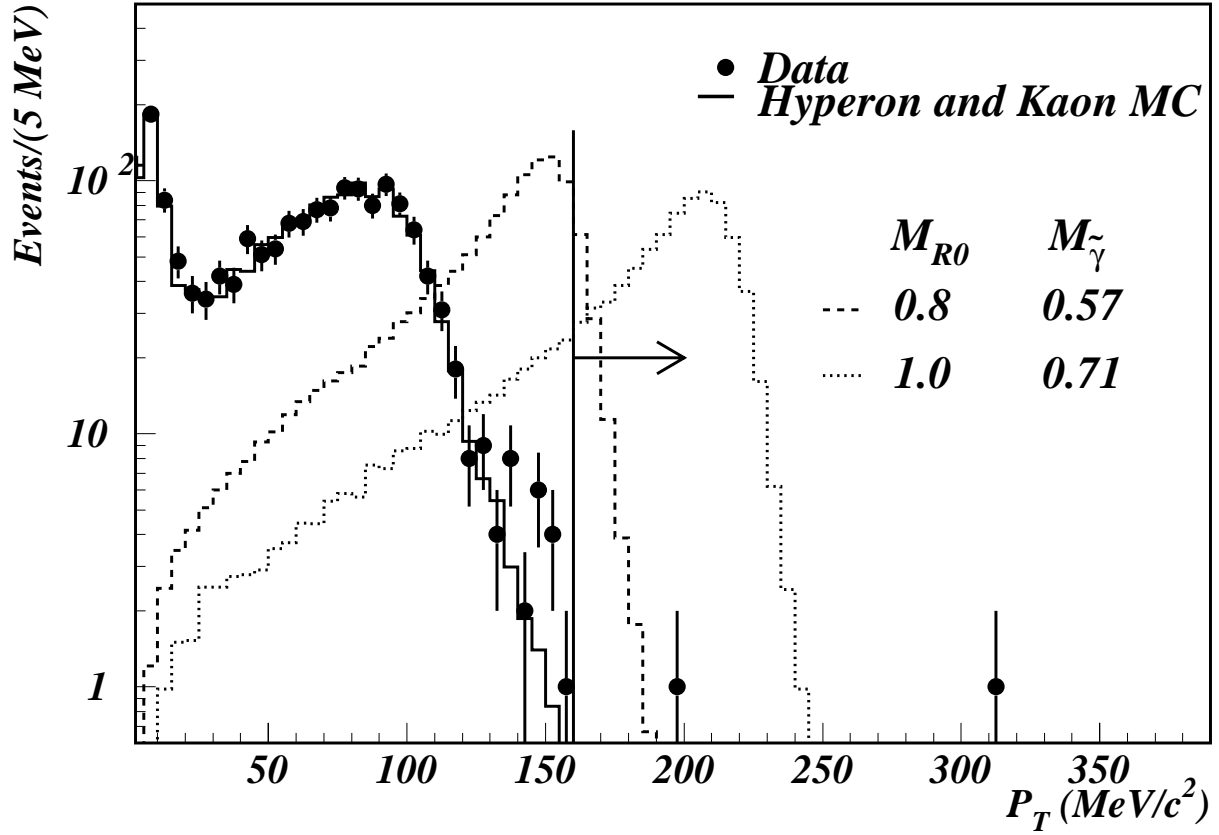


FIG. 6. The  $P_T$  distribution for  $\gamma\gamma$  events from the narrow-beam run (dots). The background from  $K_L$  and hyperon decays is shown by the solid line. The arrow indicates the  $R^0$  signal region. The MC simulation for  $M_{R^0} = 0.8, 1.0 \text{ GeV}/c^2$  (dashed, dotted lines) are also shown, both for  $r = 1.4$ .

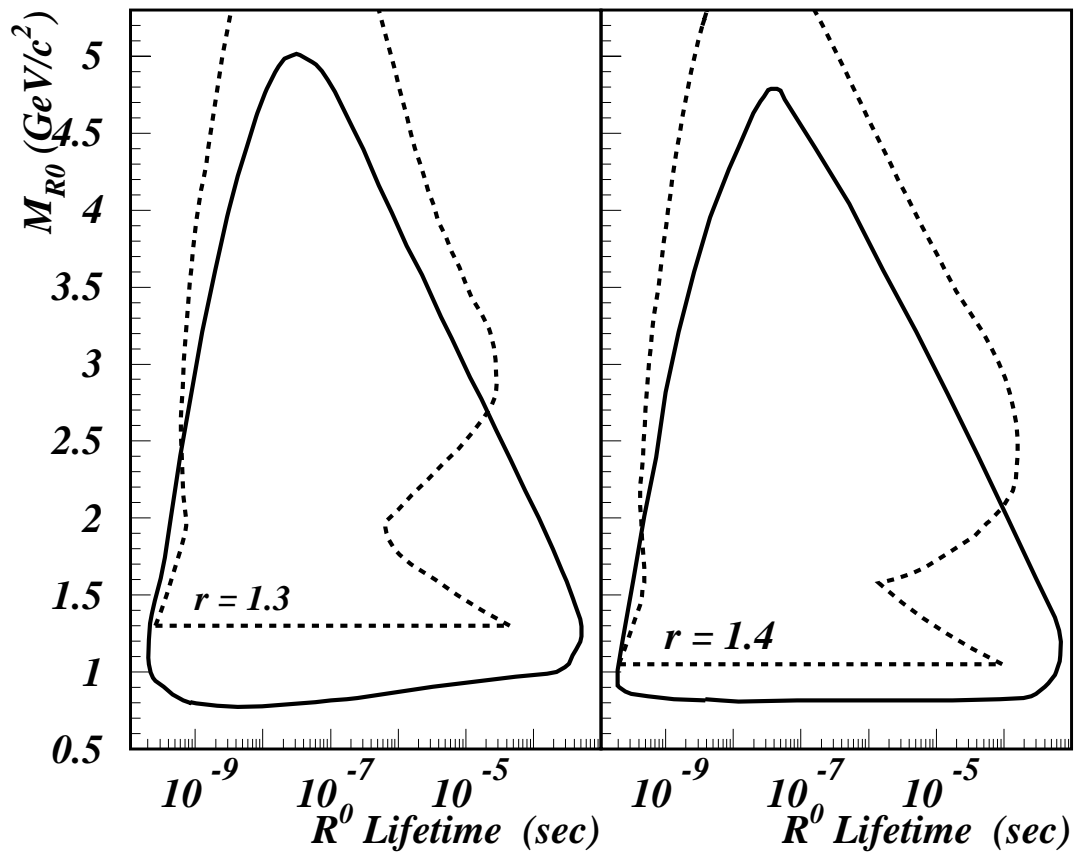


FIG. 7.  $R^0$  mass-lifetime regions excluded using pQCD for  $r = 1.3$  and  $1.4$ . The exclusion from the  $\pi^0$  analysis (solid) and  $\pi^+\pi^-$  (dashed) analysis is shown.